



Cavitation, primary break-up and flash boiling of gasoline, *iso*-octane and *n*-pentane with a real-size optical direct-injection nozzle

J. Serras-Pereira^a, Z. van Romunde^a, P.G. Aleiferis^{a,*}, D. Richardson^b, S. Wallace^b, R.F. Cracknell^c

^a Department of Mechanical Engineering, University College London, UK

^b Jaguar Advanced Powertrain Engineering, Coventry, UK

^c Shell Global Solutions (UK), Ltd., Thornton, UK

ARTICLE INFO

Article history:

Received 27 June 2009

Received in revised form 10 March 2010

Accepted 11 March 2010

Available online 20 March 2010

Keywords:

Direct-injection

Atomisation

Cavitation

Flash boiling

Optical injector

ABSTRACT

Improvements to the direct-injection spark-ignition combustion system are necessary if the potential reductions in fuel consumption and emissions are to be fully realized in the near future. One critical link in the optimization process is the design and performance of the injectors used for fuel atomization. Multi-hole injectors have become the state-of-the-art choice for gasoline direct-injection engines due to their flexibility in fuel targeting by selection of the number and angle of the nozzle holes, as well as due to their demonstrated stability of performance under a wide range of operating conditions. Recently there has been increased attention devoted to the study of the flow through the internal passages of injectors because of the presence of particular fluid phenomena, such as large-scale vortical motion and cavitation patterns, which have been shown to influence the characteristics of primary break-up. Understanding how cavitation can be used to improve spray atomisation is essential for optimizing mixture preparation quality under early injection and stratified engine operating conditions but currently no data exist for injector-body temperatures representative of real engine operation, particularly at low-load conditions that can also lead to phase change due to fuel flash boiling. This paper outlines results from an experimental imaging investigation into the effects of fuel properties, temperature and pressure conditions on the extent of cavitation, flash boiling and, subsequently, primary break-up. This was achieved by the use of a real-size transparent nozzle of a gasoline injector from a modern direct-injection combustion system. Gasoline, *iso*-octane and *n*-pentane fuels were used at 20 and 90 °C injector-body temperatures for ambient pressures of 0.5 and 1.0 bar in order to simulate early homogeneous injection strategies for part-load and wide-open-throttle engine operation.

© 2010 Elsevier Ltd. All rights reserved.

1. Introduction

The most common occurrence of cavitation is found in flowing liquid systems where hydrodynamic effects result in regions of the flow experiencing a pressure, which falls below the vapour pressure of the liquid. Reynolds was among the first to attempt to explain the unusual behaviour of ship propellers at the higher rotational speeds that were being achieved in the late 19th century, however it was Parsons in 1906 who first recognized the role played by vaporisation and conducted the first experiments on 'cavitation' [1].

It has been known for some time that cavitation phenomena occur inside Diesel injector nozzles; these have been studied in order to optimize the spray characteristics which are critical with respect to pollution formation from Diesel combustion [2,3]. Diesel injector technology has illustrated the benefits of increasing fuel pres-

sure on atomisation and this has led to the development of multi-hole injectors for gasoline direct-injection spark-ignition (DISI) engines. Although the global advantages of multi-hole DISI injectors have been established, little is understood about their spray formation mechanisms. For example, cavitation has also been associated with gasoline DISI injectors; their different operating conditions to those of Diesel engines however, means that to understand spray formation and mixture preparation it is also important to study fuel flow inside the nozzles of such injectors.

Most previous studies have focused on cavitation imaging in optical models of Diesel nozzles, typically enlarged 20×, with few studies on real-size nozzles [6–21]. Moreover, only limited work can be found on quantitative flow data in scaled-up or real Diesel and gasoline injectors, e.g. PIV work by Aleiferis et al. [4,5] in 10× and 20× models and by Tropea and co-workers or Hargrave and co-workers in real-size geometries of Diesel and gasoline injectors, respectively [11–15]. Some of the research conducted in real-size and model injectors with optical access has led to questions as to whether cavitation phenomena in injectors are directly

* Corresponding author. Tel.: +44 0 20 76793862; fax: +44 0 20 73880180.

E-mail address: p_aleiferis@meng.ucl.ac.uk (P.G. Aleiferis).

Nomenclature

ASOI	after start of injection	μ_L	dynamic viscosity of liquid
ASTM	American society for testing and materials	ρ_L	density of liquid
CAD	computer aided design	σ	surface tension
DISI	direct-injection spark ignition	p_∞	reference pressure
DVPE	dry vapour pressure equivalent	p_g	gas pressure
Ca	fluid dynamics cavitation number	p_{inj}	injection pressure
CN	pressure ratio cavitation number	p_v	vapour pressure
cr	critical (as subscript)	Re	Reynolds number
D	nozzle outlet hole diameter	T_∞	reference temperature
l	characteristic length	U_∞	reference velocity
L	length of nozzle hole		

scalable, even when Reynolds and cavitation numbers have been matched on models. Arcoumanis et al. [19] made a comparison between large-scale and real-size Diesel nozzles and found that cavitation in models occurred in the form of foamy clouds of bubbles, similar to those of Soteriou et al. [21]; in real-size injectors though, cavitation appeared in the form of large clear voids, similar to those of Chaves et al. [6]. Such results suggest that the nature of cavitation inception may change in scaled-up models and that bubble scaling factors are not well understood. Another issue of scaling is how to anticipate cavitation in one liquid, based on data obtained from another; since nuclei play an important role, scaling from one fuel to another would be tentative. Examples of different liquids used for such investigations have been Diesel oils, calibration oil, unspecified hydrocarbon mixtures, white spirits and gasolines, all of which can have widely different transport properties such as viscosity, surface tension and vapour pressure. Moreover, proper study of the effect of cavitation on atomisation might require simultaneous matching of the Weber number too which complicates the problem further.

Although studies of cavitation have been carried out in real-size Diesel injectors with optical access, previous work in real-size DISI injectors is limited and has focused on single-hole pressure-swirl atomisers [13–16]. These studies showed that the swirl flow generates a vortex in the nozzle after the pintle opening, which begins at the nozzle's exit and draws a swirling aircore (cavitation) into the nozzle hole until it attaches to the pintle. This aircore forces the exiting fuel into a thin annular region close to the nozzle walls, which becomes thinner along the nozzle, increasing its velocity. A clear wave-like structure in the flow was also identified and attributed to the radial component imparted by the contraction from the reservoir into the nozzle. In general cavitation was always found to produce a more broken-up spray, however in extreme cases examined by Allen et al. [13] in pressure-swirl atomisers, cavitation filled the entire nozzle resulting in hydraulic flip, which effectively reduced the atomisation ability of the nozzle. The rapid transitions from the initial onset of cavitation to the complete saturation of the nozzle showed the process to be highly unstable and difficult to control.

Recently, Gilles-Birth et al. [17,18] investigated the effect of cavitation in multi-hole DISI injectors using unleaded gasoline. They used a real injector coupled to a real-size optical nozzle with a single angled orifice 0.2 mm in diameter. They identified three types of cavitating structures, bubble, film and string cavitation. The latter was found for nearly all operating conditions and started at the injector needle due to strong rotational flow at the nozzle inlet, growing towards the nozzle exit but was very unstable and in its development, shape and shot-to-shot repeatability. Film cavitation and supercavitation were the dominant modes, the former observed to have stronger regions on the top side of the nozzle as bubbles were created at the nozzle inlet and flushed away and

the latter used to define conditions where bubbles completely filled the nozzle.

Apart from a recent study on flash boiling inside pressure-swirl injectors by Moon et al. [16] which will be discussed in the Section 3 of this paper, none of the previous studies on optical injectors were extended to compare various fuels, temperatures or examine flows at conditions close to flash boiling. However, such phenomena are very important because DISI injectors are mounted in the engine head and experience a wide range of operating conditions. For example, temperature effects on cavitation may not be important as long as the vapour pressure is small compared to the downstream pressure, however at injector temperatures $>70^\circ\text{C}$ and in-cylinder pressures <0.5 bar, changes in vapour pressure and vapour/liquid density become significant and no experimental results exist to explain such effects in multi-hole type nozzles. Some models have been developed to predict cavitation and its effects on sprays, but only models of limited applicability exist for multi-component fuels and flash boiling. Moreover, knowledge of the form of cavitation, i.e. bubbles or voids, is important for modellers.

1.1. Cavitation number

The spray characteristics of gasoline injectors depend not only on the physics of atomization of the liquid jet but also on the levels of turbulence generated by the internal flow upstream of the nozzle exit, as well as the extent to which cavitation occurs inside the nozzle passage. Decoupling these competing effects is not trivial. The cavitation number, Ca , has typically been used to characterize the sensitivity to cavitation in a particular nozzle arrangement and is defined as:

$$Ca = \frac{p_\infty - p_v(T_\infty)}{\frac{1}{2} \rho_L U_\infty^2} \quad (1)$$

where p_∞ is the pressure at a reference point in the flow, p_v is the vapour pressure of the liquid at the reference temperature T_∞ , ρ_L is the liquid density and U_∞ is the characteristic velocity at the reference point.

All flows will have some value of Ca whether cavitating or not. At large values of Ca , flows will be single-phase due to either p_∞ being very large compared to $p_v(T_\infty)$ or the flow velocity U_∞ being very small. As the cavitation number decreases however, nucleation will first occur at some value of Ca dependent on experimental conditions and fluid properties. This is usually denoted as incipient cavitation and defined by a critical cavitation number Ca_{cr} . Further reduction in the cavitation number below this value will cause an increase in the number of vapour bubbles. The rate growth of bubbles is radically affected by the thermodynamic properties of the liquid and vapour, which are also functions of the temperature of the liquid. Consequently the value of Ca_{cr} will

also depend on the liquid temperature. As we will see later these fundamental relationships are significant in the current application but have yet to be recorded or characterized fully in real-sized gasoline injector nozzles. Viscous effects are also important and are characterized by the Reynolds number, $Re = \rho_L U_\infty l / \mu_L$, where ρ_L is the density, μ_L is the dynamic viscosity and l is a characteristic length scale (typically the nozzle hole diameter D for injectors).

In a hypothetical flow where the liquid cannot resist any tension, vapour bubbles would appear immediately when p reaches p_v . However, nucleation does not typically happen instantaneously due to the varying levels of nuclei present in the test liquid – from contaminant gas or otherwise – and the fact that growth rates are finite, requiring a certain ‘residence time’ when $p < p_v$. Most engineering flows are also typically turbulent and unsteady. Vortical motion can occur not only because it is inherent in turbulent eddies but also because of the presence of both free and forced shedding vortices [1]. The implications for cavitation are that velocities in the centre of a vortex may reduce the local pressure to values below the mean pressure in the flow, resulting in local nucleation at the centre of that vortex. This is particularly relevant inside injector nozzles where the flow can have free vortex motion by design and/or because it must turn round sharp radii at the inlet of the nozzle which can result in significant re-circulation zones

being established just inside of the nozzle hole [4]. The latter is usually referred to as the turbulence effect [1].

In summary, there are a number of factors that affect the value of Ca_{cr} as follows:

1. Tensile strength in the fluid reduces Ca_{cr}
2. Residence time effects can reduce Ca_{cr}
3. Contaminant gas can increase Ca_{cr}
4. Viscous effects contribute to Ca_{cr} dependence on Re
5. Turbulence effects can increase Ca_{cr}

This implies that certain parameters should be controlled as much as possible in cavitation experiments, namely the cavitation number, Ca ; the Reynolds number, Re ; the liquid temperature, T_∞ and ideally the liquid quality in terms of amount of dissolved gas and the turbulence, as well as the quality of the solid boundaries and surface roughness which may affect the hydrodynamics. Of course achieving all of these is nearly impossible, however all of these must be at least considered when comparing data from different researchers or experimental arrangements. In addition, certain matching of the Weber number would also be needed for those studies involving imaging of both the cavitation and atomisation processes.

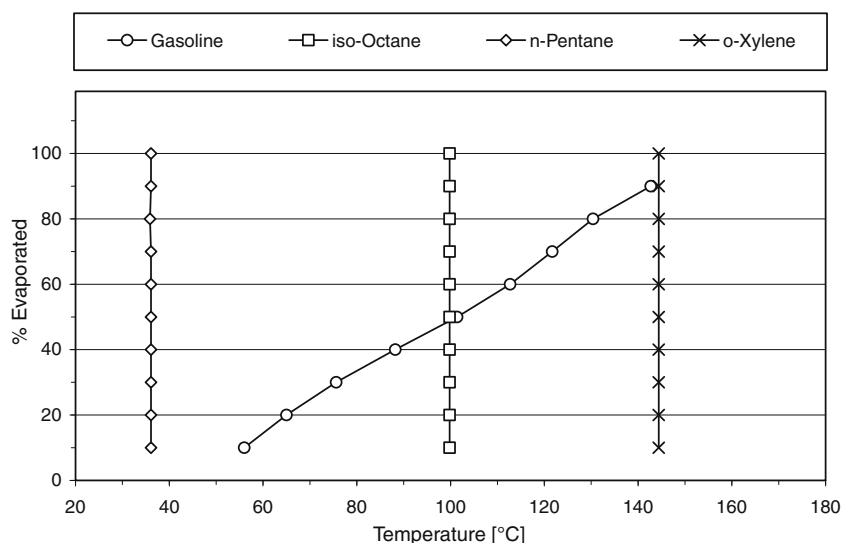


Fig. 1. Fuel distillation curves.

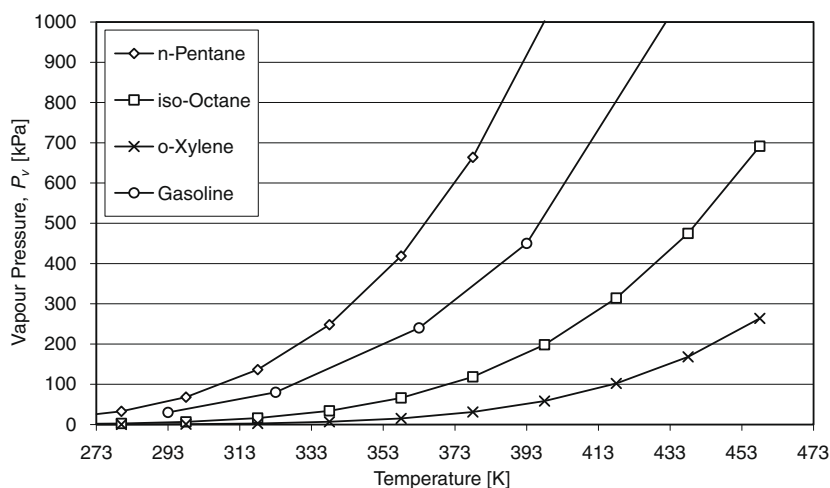


Fig. 2. Vapour pressures.

The complexities described above mean that attempts to account for changes in the scale of experiments can be problematic, residence time effects are critical in unsteady flows and nuclei size relative to the scaled model vis-à-vis a real-size nozzle will also be different. Even attempts to match the Re by changing speed may lead to confusion due to effects on the residence time as well as altering the cavitation number. The pressure can be changed to recover the cavitation number, but this can then alter the nuclei content; surface roughness is also difficult to match using different materials. Finally, fluid transport properties have different temperature and pressure relationships which are typically non-linear. The use of a global transition regime map from non-cavitating to cavitating flows is therefore difficult to build up. On a positive note however, the above parameters are all much less sensitive when cavitation is already fully developed, justifying the continued use of the cavitation number and the Re number as the two most widely used non-dimensional parameters for such studies.

A range of critical cavitation numbers which define the cavitating transition have been quoted in the literature relating to Diesel injectors for a variety of nozzle-hole geometries and injection parameters. However, the most popular definition of a cavitation number for injection phenomena has not been that shown in Eq. (1) but the following:

$$CN = \frac{p_{inj} - p_g}{p_g - p_v} \quad (2)$$

where p_{inj} is the injection pressure, p_g is the gas pressure and p_v is the vapour pressure. This is not strictly correct from a fluid dynamics perspective but makes comparisons with data from different experimental arrangements simpler, since the effect of flow velocity is eliminated and only experimental conditions relating to injection, gas and vapour pressures are considered, i.e. the ratio of forces that support versus those that suppress cavitation. Critical cavitation numbers (or incipient cavitation numbers) based on this definition have been found to fall in the range of 0.5–10, with associated critical Reynolds numbers of between 5000 and 30,000 [2,3,9,13,15,18].

1.2. Present contribution

The effects of cavitation and flash boiling on spray primary break-up were investigated for different fuels and operating conditions. This was achieved using a real-size optical nozzle to simulate the flow in one of the holes of a real multi-hole injector previously used by the authors for macroscopic spray imaging and related engine studies [22–27]. These studies showed that the geometry and break-up of sprays from such injectors is significantly affected by operating conditions, which result in a high degree of superheating of the fuel components, i.e. conditions of high liquid temperatures and low gas pressures. However, there is still a limited understanding of the mechanisms leading to these effects and limited experimental data which clarifies the role that liquid transport properties such as surface tension (σ), viscosity (μ), density (ρ), boiling point and vapour pressure (p_v) have on in-nozzle phenomena and overall spray development. This is complicated further by the wide operating envelope of gasoline engine injectors which must inject fuel at conditions of low ambient pressure, typically from ~ 0.2 to ~ 5 bar or more, and at liquid temperatures of -10 °C or lower, to over 150 °C at the injector tip under high-load firing conditions. There are also no experimental results of the interactions between cavitation and flash boiling at extremes of pressures and temperatures using real-size optical nozzles with various fuels. The current paper attempts to fill this gap in the literature by presenting results from an imaging investigation relevant to a state-of-the-art engine combustion system.

2. Experimental apparatus and procedures

The investigation used the same injection system and facilities described in previous publications by the authors [22–27]. Therefore primarily deviations from standard equipment, i.e. details pertaining to the design and use of the optical nozzle will be mainly referred to in this section.

2.1. Fuels

A standard commercial grade European gasoline was used containing several hydrocarbons, typically ~ 35 – 40% C5 or lower, similar levels of C6–C8 and the remainder C9–C10 hydrocarbon chains. On the basis of these fractions, it was decided to also investigate specific single components to aid the discussion of fuel property effects on in-nozzle phenomena and provide some interpretation of the results obtained using a standard gasoline. From typical gas-chromatography analysis data, the representative single component fuels were chosen to be *n*-pentane and *iso*-octane. The former is a typical low boiling point component found in gasoline, with boiling temperature 36.1 °C. The latter is a mid-range boiling point component with boiling temperature 99 °C. These are known to be two representative constituents in a typical European gasoline. Finally, a heavier gasoline component, *o*-xylene, with boiling temperature 144 °C was also included in the discussion of the results but was not included in the test matrix because of its lower contribution by volume and the fact that its properties make it quite insensitive to the phenomena being investigated at the main conditions of interest. The use of *o*-xylene served only to bound the envelope of gasoline's thermophysical properties, which is useful when describing the effects of different chemical species on the observed behaviour of a multi-component fuel.

The distillation curves of all single components and gasoline are shown in Fig. 1 along with vapour pressures in Fig. 2. The vapour pressures were calculated using correlations obtained from [28] within a valid temperature range for *iso*-octane, *n*-pentane and *o*-xylene. For gasoline, the vapour pressures were obtained experimentally using ASTM D5190 (dry vapour pressure equivalent, DVPE) and carried out at Shell Global Solutions (UK), Ltd. It is quite interesting to note that the vapour pressure of gasoline is biased towards the low volatility component *n*-pentane.

2.2. Injector

A multi-hole injector producing six spray plumes was used as shown in Fig. 3. The injector was designed for vertical installation on an engine head and in a close spacing arrangement with the spark plug, with plumes 1 and 6 passing on either sides of the plug, one on the intake side and one on the exhaust side. The six nozzle holes have different turning angles that direct fuel to different areas of the combustion chamber but they are symmetric with respect to a centreline, therefore, only three 'sprays' can be seen from the main imaging view corresponding to the three plume pairs (1,6; 2,5; 3,4). Further details can be found in [22–27].

2.3. Macroscopic, near and in-nozzle imaging

A pressure chamber was used to study the spray development in a quiescent environment in order to de-couple the effects of engine intake flow on atomisation and spray break-up. An image of the pressure chamber is shown in Fig. 4. The octagonal shape allows for simultaneous multi-technique characterization, including imaging with back or side lighting and the use of off-axis techniques such as phase Doppler anemometry for droplet sizing and velocity measurements. The pressure chamber arrangement also

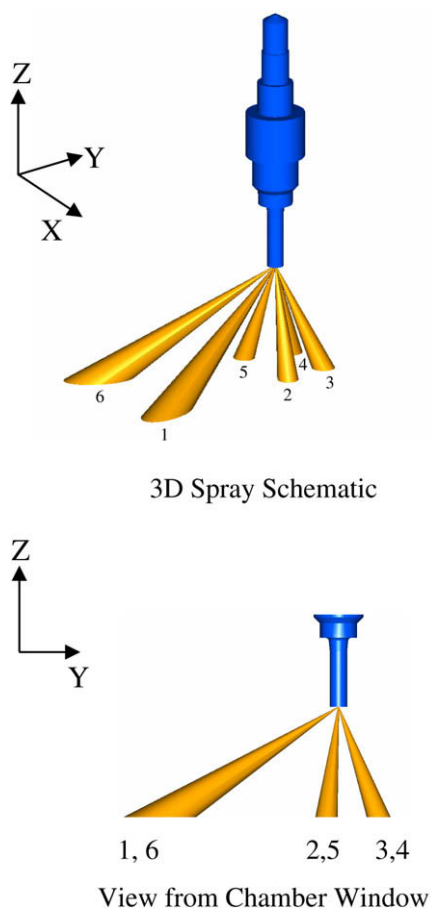


Fig. 3. Schematic of spray plumes.

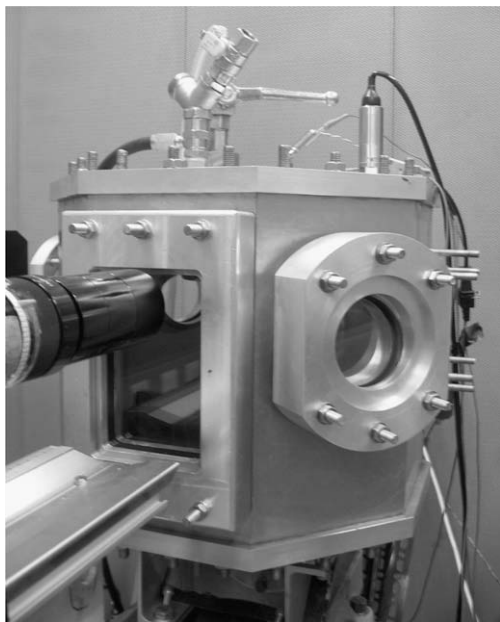


Fig. 4. Pressure chamber.

allows independent variation of fuel type, injector-body temperature, gas pressure and injection pressure. Further details about the facility can be found in [22,23].

Near-nozzle high-magnification imaging was initially carried out to visualize the ‘first fuel’ exiting the real 6-hole injector and

its ensuing spray development. The fuel spray was recorded using a Photron® APX-RS high-speed digital video camera. The camera was operated at 50 kHz frame rate, giving a temporal resolution of 20 μ s with 1 μ s integration time. A model K2/SC™ series long-distance microscope system from INFINITY was used to obtain suitable magnification. Lighting was produced using a photographic flash lamp with duration of a few milliseconds and back-lighting. For the in-nozzle imaging, the high-speed camera was operated at 9 kHz frame rate also with 1 μ s integration time.

To optimize the imaging arrangement of all pairs of plumes of the multi-hole spray, the injector was mounted at the top of the pressure chamber at an angle of 19° (with respect to the vertical axis of the chamber). For the optical nozzle arrangement that employed a single angled nozzle hole as will be shown in the next section, the injector-body was installed in a different mounting configuration that allowed fixed vertical alignment. The injector-body was heated in its mounting to replicate injector and fuel system *in situ* heating in an engine. A 150 W band heater was used around the injector mounting whilst a thermocouple sensor (installed close to the injector tip) and a temperature controller allowed accurate temperature regulation, typically for experiments within a range of 20–120 °C [22,23]. For the remainder of the paper the injector temperature will be referred to as that of the liquid in order to facilitate discussion, although the actual liquid temperature exiting the nozzle was not measured. Fuel pressure was provided by a pneumatic piston ram pump which avoided pressure fluctuations in the fuel rail. The gas pressure was also set and monitored by a pressure transducer to ensure consistency throughout experiments. Both atmospheric (1.0 bar) and sub-atmospheric (0.5 bar) gas conditions inside the chamber were investigated to simulate full-load and part-load engine conditions with early intake stroke injection strategies for homogeneous mixture formation. The gas temperature was monitored at 20 °C throughout the experiment.

2.4. Optical nozzle design

This part of the investigation was carried out using bespoke nozzles manufactured from Perspex®. A direct injector-body was used for its actuation mechanism and needle. The injector was disassembled to reveal the internal needle and a steel adaptor plate was designed and manufactured to couple the nozzle to the injector. Perspex® was chosen for the nozzle as this has a similar refractive index to iso-octane [4]. The relatively low strength of Perspex® however meant that the wall thickness had to be larger than the stainless steel from the original injector. The sides of the stem were also required to be flat to avoid refraction of the imaged light. The nozzle was attached to an adaptor and was sealed using an o-ring at the mating surface. The CAD models of the nozzle designs are shown in Fig. 5.

The outlet diameter of the real injector nozzle holes was 0.5 mm, although it is believed that internally, the injector passage can be as narrow as 0.2 mm with a step change to 0.5 mm to avoid deposit formation. However, in the absence of more detailed information on the exact geometry of the injector's internals at the time of this work, a nozzle diameter of 0.5 mm was used with 2.5 mm hole length giving an L/D of 5 for this nozzle. The hole was designed at 60° angle to the vertical as an approximate to 58.8° of plumes 1,6 of the real injector in Fig. 3. It can be seen that the nozzle in Fig. 5(a) included an initial bowl feature to spread stresses which mean that imaging the nozzle from the side would obscure the flow as it exited the nozzle; this was attempted as a first iteration following similar designs reported in [17,18]. A second design was optimized for simultaneous imaging of internal and external flow details, shown in Fig. 5(b). The transformation of the original injector to one with an optical nozzle is shown in Fig. 6. Fig. 7

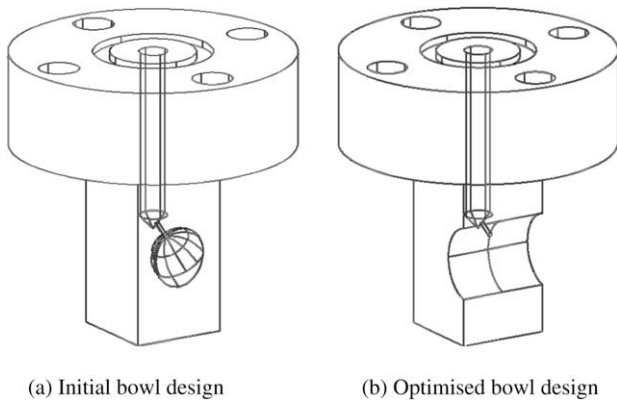


Fig. 5. Optical nozzle CAD models.

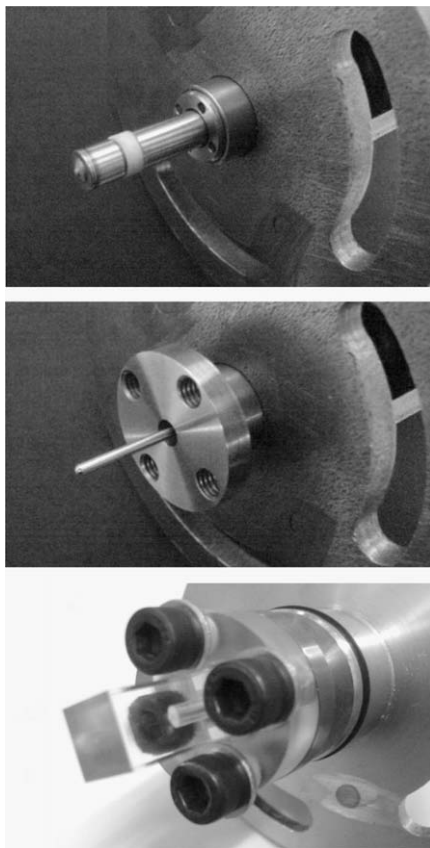


Fig. 6. Injector stem (top), needle inside adaptor (middle) and optical nozzle attachment (bottom).

shows the whole assembly ready to be mounted onto the chamber with the band heater in place.

In order to ensure consistency of results between the real injector and the optical nozzle model, flow rate measurements were taken using the optical nozzle to match the estimated single-hole flow rate from the multi-hole injector. This was based on the measured injector flow rate at the working fuel pressure (150 bar) divided by the number of nozzle holes. Although some discrepancy of flow rate for each hole is expected due to the different turning angles and other in-nozzle phenomena, it was found to be difficult in practice to measure individual hole flow rates accurately and in a time/cost effective way. The flow rate was adjusted by changing the fuel pressure. Flow rates for the optical nozzle were measured at fuel pressures of 23, 25 and 30 bar giving values of 2.81, 3.12,



Fig. 7. Optical nozzle full assembly.

3.82 g/s, respectively. The flow rate measured for the optical nozzle at 23 bar closely matched the estimated flow rate for the real injector nozzle of 2.78 g/s [22], thus allowing the matching of the Reynolds number for both nozzles. A pneumatic ram pump was used to supply the fuel pressure bar and a solenoid valve operated to allow flow through to the optical nozzle during image acquisition; the experiments were conducted under steady-state flow conditions by imaging with a fully open injector needle.

Reynolds numbers were calculated for the single component fuels using fluid properties of density and viscosity for varying temperatures along the liquid saturation curve, as shown in Fig. 8; these will be discussed later in the Section 3. The Reynolds numbers were based on a velocity of 22 m/s, as calculated from the measured flow rate and the cross-sectional area of the real nozzle's outlet hole with $D = 0.5$ mm that matched the optical nozzle's hole constant diameter along the full length of the nozzle-hole passage. However, it needs to be pointed out that the actual Reynolds number inside the real injector's nozzle-hole passage could be higher in the case of a narrower internal hole geometry, because that would lead to higher velocity from continuity. For example, considering the case of an internal nozzle hole diameter of 0.2 mm with a step change to a 0.5 mm outer hole diameter (as discussed earlier), values of Re inside the passage of 0.2 mm in diameter could be 2.5 times larger than those based on the characteristic outlet hole diameter of 0.5 mm. Calculation of spray tip velocities from the spray images of the real injector, showed values as high as 70–80 m/s at the start of injection; these are consistent with the assumption of a narrower internal passage diameter. Nevertheless, in the absence of specific information on the internals of the real injector, it was decided that within the scopes of the current publication it was adequate to base the analysis on the outlet hole Re number that the optical nozzle was designed upon and operated at. This decision was also verified by the similar relative response of the different fuels to the different operating conditions, as observed macroscopically between the real injector's and the optical nozzle's spray formation (discussed in the following section). Future work will study this issue in more detail by designing and operating optical nozzles with narrower diameter for comparison with the results of the present work and for further critical analysis.

3. Results and discussion

The results presented discuss the characteristics of the internal and near-nozzle flow phenomena relative to the liquid fuel tem-

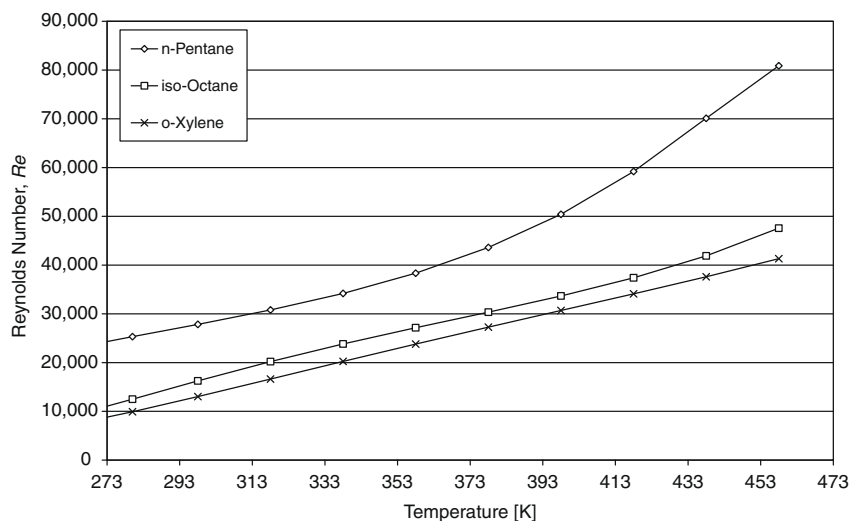


Fig. 8. Reynolds numbers.

perature, gas back-pressure and fuel properties, incorporating an analysis of cavitation and flash boiling relative to observations of the spray's primary break-up.

3.1. Macroscopic and near-nozzle imaging

Before presenting the results of the optical nozzle it is advised that the reader familiarise him/herself with the spray pattern. Images of initial and full spray development are given in the Appendix. These are shown in order to highlight features of the global primary spray break-up near the nozzle as well as to give an overview of the macroscopic spray formation brought about by changes in the operating conditions, namely spray convergence and collapse at high temperatures and low gas pressures. Images are grouped by fuels, *i.e.* gasoline, *iso*-octane, *n*-pentane, in Figs. A1, A2 and A3, respectively. Both high-magnification and macroscopic spray images are shown to aid visual interpretation. Only three plume pairs can be seen instead of the six individual spray plumes due to the symmetry of the nozzle-hole pattern in the imaged view (refer to Fig. 3).

The macroscopic sprays behave in very similar fashion at low temperature conditions and there are no clear distinguishing characteristics of break-up for the three different fuels. At 1.0 bar gas pressure, increasing the fuel temperatures has a noticeable effect for *n*-pentane in particular, with the spray plumes converging below the injector, a behaviour termed 'spray collapse', but gasoline and *iso*-octane remain very similar in appearance. At 0.5 bar gas pressure, gasoline also shows evidence of spray collapse at high temperatures but *iso*-octane is quite insensitive to such operating conditions. Further inspection showed that there were differences between the left-hand plumes (identified as 1,6 from Fig. 3), which had nozzle holes with greater turning angles compared to the other holes. Nozzle holes 1 and 6 showed less signs of macroscopic plume distortion at conditions of spray collapse which may be associated with lower levels of cavitation, since the flashing process is assumed to be similar outside all the nozzle holes, as first reported in [22,23]. Indeed the study of Gilles-Birth et al. [17,18], investigated the effect of the orientation of the nozzle hole on cavitation and a greater turning angle was found to decrease the extent of cavitation inside the nozzles.

The near-nozzle images clearly show that macroscopic characteristics are replicated immediately outside the nozzle hole for the same conditions. The sensitivity of the fuels to such conditions is illustrated by the differences in individual plume cone angles

(larger at high temperatures due to plume swelling), overall cone angles (lower at higher temperatures due to spray collapse drawing the plumes close together under the injector tip), liquid penetrations (only marginally lower at high temperatures) and interactions with the gas phase (larger at high temperatures due to improved break-up and atomisation, which lead to smaller droplets being entrained into the recirculating flow adjacent to the spray plumes).

For all fuels, the 'first' spray tip seen at the nozzle is very similar for all conditions, time *t*. Individual plumes are clearly discernible with clear separation between them. However, at *t* + 20 μ s, the trends exhibited by the global spray form are already evident. At conditions of spray collapse the plumes can be seen to widen on exit from the nozzle hole, particularly clear for *n*-pentane. This could suggest that in the first frame, at the first stages of needle lift, the flow is not yet fully established within the nozzle, resulting in the observed similarities between conditions and fuels.

All of the observations suggest that even at conditions where pure flash boiling would be expected, *e.g.* *n*-pentane at 120 °C and 0.5 bar gas pressure, this clearly does not occur but the plumes are swelled to over two and three times the nozzle hole diameter. This expansion could arise from the vapour generated inside the plumes by rapid evaporation of the fuel, however it can also suggest the presence of expanding vapour bubbles originating from inside the nozzle *i.e.* the fuel does not simply 'flash boil' upon release into the atmosphere, but the process of 'boiling' begins inside the injector. Although the effect of two-phase flow inside the nozzles has been shown to affect primary break-up [6,17,18] and spray cone angles, the coupling with flash boiling is not well understood and must be investigated further in optical nozzles.

3.2. Cavitation numbers and mass flow rates

The likelihood of cavitation in the injector under study was examined by comparing nozzle flow rates with data presented by Gilles-Birth et al. [18]. When flow rate was plotted against back-pressure by the latter authors, the onset of cavitation was illustrated by the onset of a 'choked' flow regime where there was no further increase in flow rate with reduction in back-pressure. Specifically, with a reduction in gas pressure from 16 to 10 bar, there was a linear increase in flow rate from approximately 3.5–5.0 mm³ per injection event, (for a pintle opening time of \sim 1.0 ms). Any further decrease in gas pressure maintained the flow rate between 5.2 and 5.5 mm³ per injection event. For the multi-

hole injector examined in the current study the flow rate per nozzle hole over 1 ms would equate to $\sim 5\text{--}5.2\text{ mm}^3$ at 20°C and 1 bar gas pressure [22]. This value's proximity to the trends of Gilles-Birth et al. [18] suggested operation of the current nozzle very close to the onset or inside the cavitating regime; increasing the pressure drop across the nozzle (i.e. reducing the gas pressure, p_g ; or increasing the injection pressure, p_{inj}) would increase the severity of cavitation.

The cavitation numbers (CN) for a range of liquid temperatures were calculated to aid interpretation of the results. These were plotted for the same fuels presented in the vapour pressure graph and are shown in Figs. 9 and 10. Values were calculated from Eq. (2). The effect of operating at gas pressures in the range of the fuels' vapour pressures (Fig. 2), means that the value of the denominator becomes very small and therefore the values of CN are orders of magnitude higher than those reported in [17,18] for similar geometry nozzles. The effects of temperature also appear in the CN via the vapour pressure/temperature relationship, but the low gas pressures used in this study exacerbate these effects and at higher temperatures the vapour pressures become higher than the gas pressures, leading to negative values of CN. Only CN values up to this transition point have therefore been

plotted for clarity. Cavitation numbers at higher gas pressures are considerably lower as shown in Fig. 9 but still much higher than those reported in [17,18]. The most striking feature of Fig. 9 is the trend for gasoline, which is incredibly sensitive to temperature, compared to *iso*-octane. This derives from its vapour pressure relationship, which is biased towards *n*-pentane rather than *iso*-octane (Fig. 2). Given that *iso*-octane is commonly used as a substitute for gasoline in many engine research applications, the results of in-nozzle and primary break-up imaging together with the above results indicate that for realistic operating conditions at elevated temperatures, multi-component fuel behaviour should not be approximated to a single component fuel unless a comprehensive sensitivity study has been previously carried out that justifies such an action. Failure to do so can lead to serious underestimation of particular fluid dynamic effects on processes of spray break-up and evaporation. This is particularly relevant for spray and engine modellers who seldom have the luxury of modelling a complete gasoline blend and need to choose representative single components. This analysis suggests that using fluid properties that are closer to *n*-pentane than *iso*-octane might result in better modelling accuracy for the purposes of real fuel injection processes.

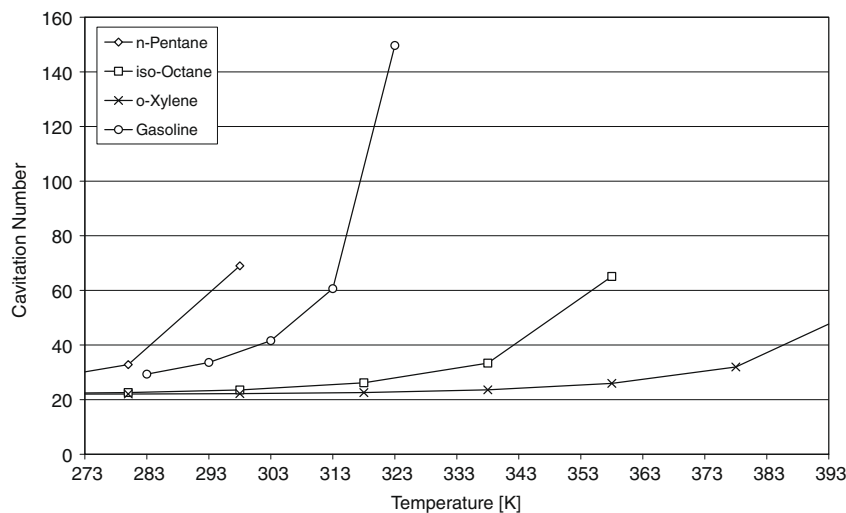


Fig. 9. Cavitation numbers (1.0 bar).

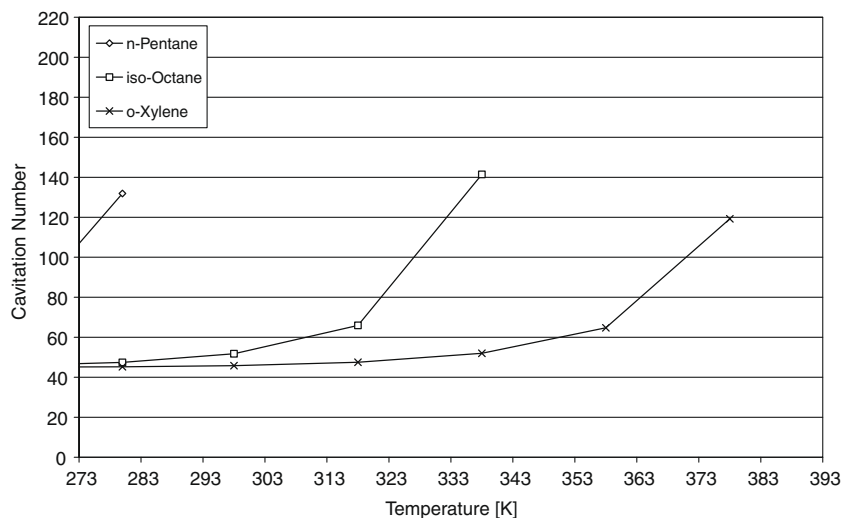


Fig. 10. Cavitation numbers (0.5 bar).

Gilles-Birth et al. [17,18] used an injector-body coupled to an optical nozzle with a single angled nozzle hole (0.2 mm in diameter, 0.5 mm hole length *i.e.* $L/D = 2.5$), gasoline fuel at 20 °C, injection pressures of 20–40 bar and high gas pressures in the range 1–16 bar. A range of critical cavitation numbers (defining the transition from non-cavitating to cavitating conditions) were quoted in [17] from the literature relating to Diesel injectors, for a variety of nozzle-hole geometries and injection parameters. This information is replicated in Fig. 11 showing the range of critical cavitation numbers (CN_{cr}), based on the definition of Eq. (2). Test cavitation numbers corresponding to the conditions used in the current investigation are also superimposed for 0.5 and 1.0 bar gas pressure. Other points are also included, *e.g.* for 5 and 12 bar to simulate stratified conditions in an engine (when fuel is injected in the compression stroke), however these conditions were not included in the current test matrix and are shown for reference only. Figs. 9 and 10 show that the lowest cavitation numbers in the current investigation ranged from $CN = 22$ at 1.0 bar to $CN = 45$ at 0.5 bar for *iso*-octane at 20 °C (293 K), with gasoline's CN shifted to much higher values.

Even accounting for variations in the transition regimes between nozzles with geometrical differences, these larger cavitation numbers compared to the values of 0.6 and 0.8 reported in [17] suggested from the outset that the real injector nozzle of the present study was operating well inside the cavitation regime at the conditions considered. The optical nozzle work aimed at observing and analysing the mechanisms of phase change inside the injector.

3.3. Nozzle A

Images of cold and hot fuel flow at 1.0 and 0.5 bar gas pressure are shown in Fig. 12 from the database of the current study. Note that these images were captured using the bowl cut-out in the optical nozzle, Fig. 5(a), and hence the initial emergence of spray from the nozzle is obscured. The spray slightly downstream of the nozzle exit, as well as the flow in the nozzle channel however, can be clearly seen.

In general, a dark region is seen along the top of the nozzle passage, suggesting the presence of vapour in this region, as liquid fuel is translucent due to the similar refractive indices of Perspex® and fuel; liquid therefore is identified by clear regions as those seen in the lower parts of the nozzle. Under close analysis it is clear that the dark regions at the bottom of the nozzle passage where the channel meets the bowl, appear to be larger with increased fuel temperatures. This effect is augmented if the gas pressure is fur-

ther reduced to 0.5 bar. At 1.0 bar gas pressure with hot fuel, the dark region at the bottom of the channel is larger around the nozzle exit than at 20 °C. Although the spray produced is not dramatically affected by this temperature difference the hot spray is generally wider (larger cone angle due to plume swelling) and in particular has more pronounced break-up along the top side of the imaged plume. Gilles-Birth et al. [18] has also found that cavitation produced a less well-defined, more broken spray.

It is known that the effects of collapsing cavitation bubbles outside the nozzle can contribute to spray break-up and this seems to occur even at 20 °C; for hot conditions at the same gas pressure, it is likely that this collapse has an increased effect on the spray break-up as a result of different fluid properties *e.g.* lower surface tension, viscosity and higher vapour pressure, which all support faster bubble growth rates. The darker spray for hot conditions probably also indicates a higher concentration of vapour within the liquid fuel and/or higher droplet concentration within the spray, as cavitation bubbles expand and burst rather than collapse, thus the swelling seen in the primary break-up. These observations are compatible with similar plume 'swelling' noticed in the macroscopic imaging.

At the hot fuel, low-pressure condition, the dark region along the bottom of the channel has expanded nearly a quarter to a third of the length into the nozzle and the subsequent spray is seen to be severely affected within the distance of the cut-out bowl (~2 mm). Cavitation structures, however do not appear to be that different compared to the 1.0 bar condition within the spatial resolution of the experiment. This is not altogether unsurprising since cavitation inside the nozzle will be governed mainly by liquid temperature, through its effect on the vapour pressure. Although gas back-pressure also affects cavitation and is included in the definition of cavitation number in Eq. (2), the CN at these conditions become somewhat meaningless since the vapour is much greater than the gas pressure, resulting in negative values of CN . The relative difference between the vapour pressures at high temperatures and for a 0.5 bar change in gas pressure therefore has a small effect on the CN .

The effect of low gas pressure is demonstrated strongly outside the nozzle by two mechanisms; the first is the lower resistance to vapour bubble growth and the second is the reduction of the liquid boiling point and automatic increase in the level of superheat experienced by the fuel constituents. The result is rapid bursting of vapour bubbles within the spray upon exit causing the enhanced disintegration of the jet. This dramatically improves atomization and 'destroys' the nominal 'solid'-core structure. The increased levels of superheat also drives the rapid evaporation process of the

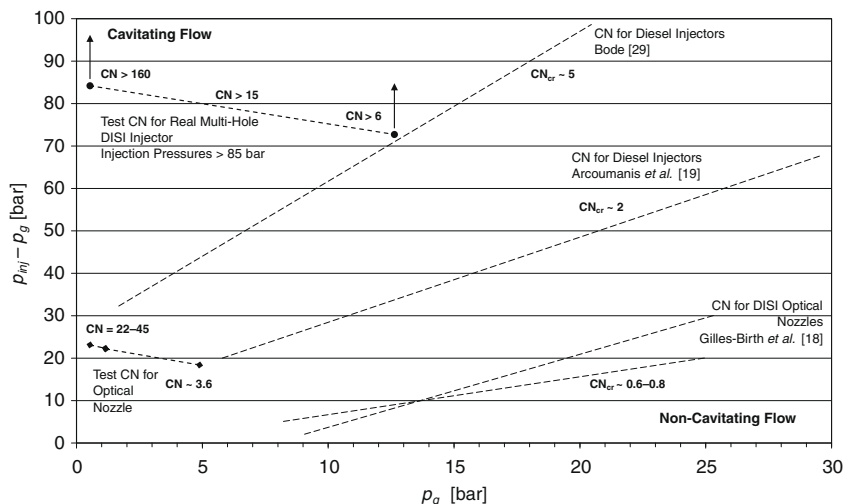


Fig. 11. Critical cavitation numbers reported in the literature with current test cavitation numbers for *iso*-octane at 20 °C superimposed. Adapted from [17]. (See above-mentioned references for further information.)

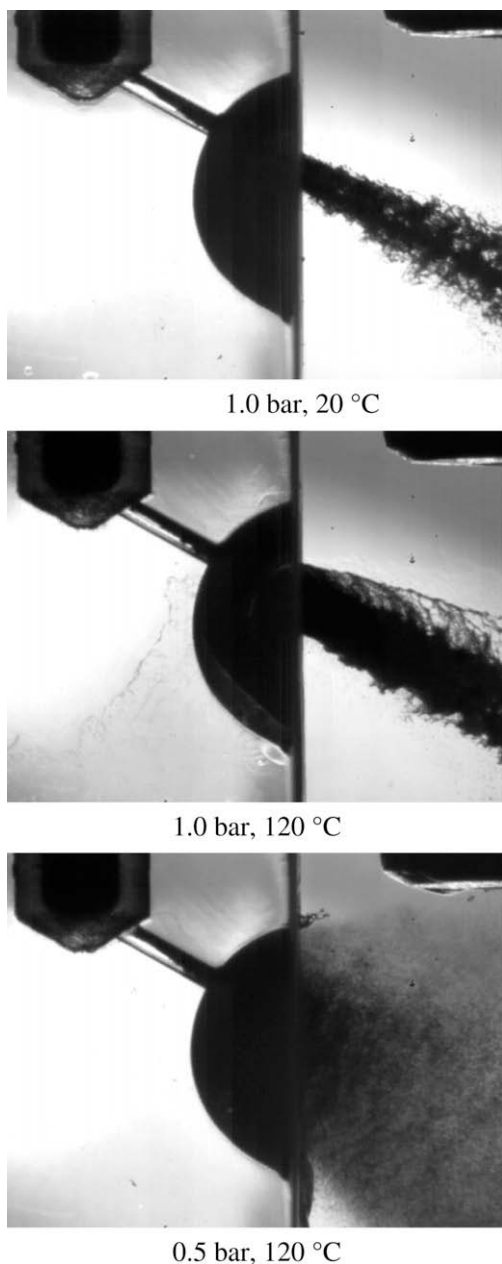


Fig. 12. Bowl nozzle using gasoline.

newly formed ligaments and droplets, so that fine atomization is nearly instantaneous.

Nozzle A proved to be successful in allowing cavitation and initial spray formation to be imaged, however, the presence of the cut-out bowl made it unclear as to how the bowl itself interfered with the spray formation process, particularly at the extreme conditions of pressure and temperature; therefore a second nozzle design iteration was used to improve the experimental arrangement, confirm these effects and allow a more detailed study of the effects of fuel properties on primary break-up.

3.4. Nozzle B

The modified optical nozzle shown in Fig. 5(b), in which the original cut-out bowl had been elongated to produce a groove, thereby allowing complete imaging of the spray at the exit of the nozzle hole, was used to capture the image groups shown in Figs. 13–15 for gasoline, *iso*-octane and *n*-pentane, respectively.

Since the imaging of the nozzle channel was unchanged using this new nozzle design, in general the same features discussed for Nozzle A apply for Nozzle B using gasoline. However, the fuels will be discussed individually first before direct comparisons are made between their primary break-up characteristics. The highest temperature to be discussed with this nozzle is 90 °C because 120 °C was too high for any useful relative comparison of the phase change characteristics of all three fuels at both 1.0 and 0.5 bar.

In Fig. 13, the effect of gas pressure reduction from 1.0 to 0.5 bar is quite small for gasoline at 20 °C. There is a slightly wider spray for the 0.5 bar condition and the levels of cavitation inside the nozzle are comparable. At these conditions the cavitation zone never reaches the lower part of the nozzle down to the exit plane. Although difficult to reproduce in hard-copy format, movies of the high-speed imaging sequence showed that the periodicity in spray break-up was also comparable in frequency, suggesting similar in-nozzle dynamics. At 90 °C, the levels and locations of cavitation again appear very similar for the 0.5 and 1.0 bar gas conditions. However, the sprays show quite obvious differences. At 0.5 bar, the spray cone angle is far greater than any of the other conditions and the fuel begins to atomize immediately outside the nozzle. The spray is also asymmetric with the angle on the top of the plume being larger than the bottom; notice the top side of the nozzle is also where cavitation is present. This observation is consistent with other investigations which have found that spray cone angles are larger in locations where cavitation develops [18]. The increased levels of flash boiling at low gas pressures are also seen to reduce the liquid length significantly and in fact within only 4–6 nozzle diameters the spray ‘core’ is no longer intact and the backlight is clearly visible through the atomized spray. This is in clear contrast to the 1.0 bar gas condition which even at 90 °C shows a much narrower jet exiting the nozzle. The asymmetry of the top side of the plume is also noticeable but the cone angle is smaller than that for 0.5 bar gas pressure, although still wider than at 20 °C.

In Fig. 14, the behaviour of *iso*-octane is clearly less sensitive to operating conditions than gasoline in general. There are no obvious differences in the initial sprays produced or in the mechanisms of primary break-up. Levels and locations of cavitation are generally similar for all conditions but there are differences from 20 °C to 90 °C. Although cavitation fills the nozzle hole more at high temperatures, there does not appear to be an obvious effect on the spray formation. From the observations of gasoline, this indicates that the levels of superheating of the fuel components contribute more towards the rapid jet disintegration and atomisation than levels of cavitation in isolation, since cavitation levels or structures are not that dissimilar to those of gasoline. It would be interesting to reproduce the results in a similar but non-cavitating nozzle in order to fully de-couple the effects of cavitation and flash boiling on spray formation. Whether this is possible while maintaining *Re* the same would require further investigation, possibly by using rounded inlet holes or conical hole geometries in order to suppress cavitation at these conditions.

The results for *n*-pentane in Fig. 15 show similar spray formation at 20 °C compared to gasoline and *iso*-octane. However, there are potentially greater levels of phase change near the nozzle exit compared to the other fuels, but no significant differences in the primary break-up. With the current spatial resolution it is difficult to make further informed analysis on the nature of the structures of cavitation between the three fuels, particularly at 20 °C. At 90 °C however, *n*-pentane shows clear differences in the levels of cavitation, with black regions nearly completely filling the nozzle hole at both 1.0 and 0.5 bar gas pressures. In terms of spray formation, primary break-up is nearly instantaneous and atomisation is dramatically improved relative to either gasoline or *iso*-octane with the jet disintegrating rapidly into small ligaments and fine droplets.

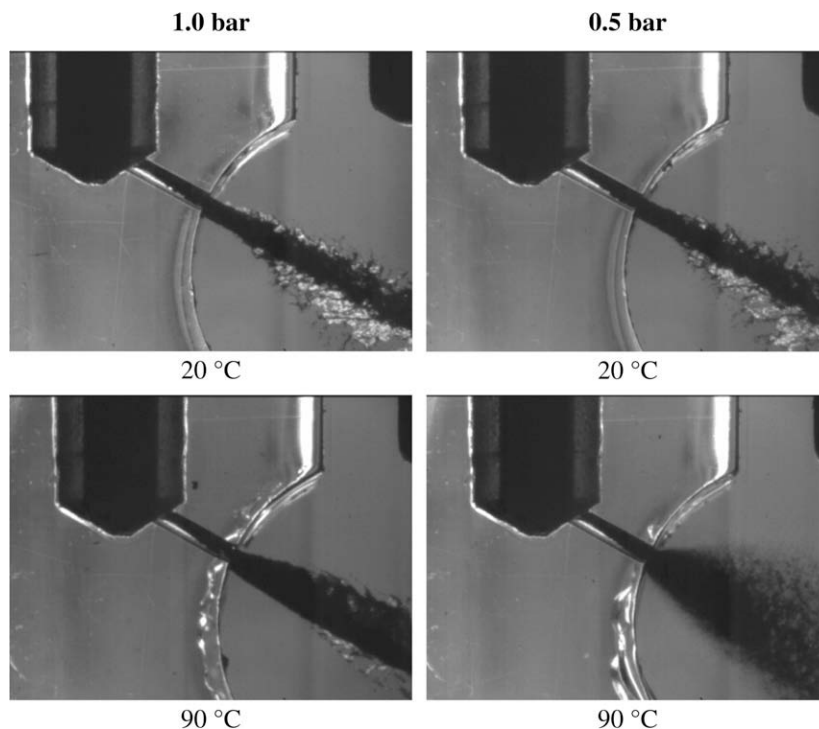


Fig. 13. Gasoline at different pressure and temperature conditions.

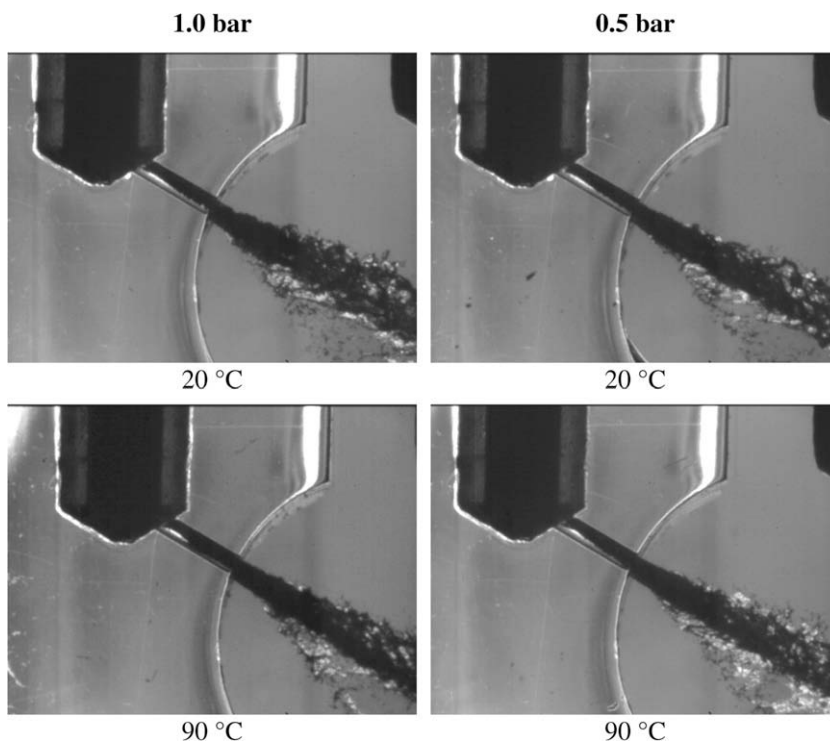


Fig. 14. Iso-octane at different pressure and temperature conditions.

There are also striking similarities in the atomisation of *n*-pentane at 90 °C, 0.5 bar and gasoline 120 °C, 0.5 bar shown in Fig. 12, although interestingly cavitation is observed to be much less with gasoline. This appears to be further evidence that as a mechanism of atomisation enhancement, cavitation may not play as important a role compared to the levels of superheat experienced by the fuel components.

At 1.0 bar gas pressure, *n*-pentane shows excellent atomisation once again and cavitation levels appear comparable to those at 0.5 bar, however the cone angle is smaller and there is once again some directionality in the spray. Differences in the spray formation should therefore stem from the lower levels of superheat as a result of the higher boiling point at 1.0 bar. Although the hierarchy of mechanisms is difficult to define because cavitation and flash

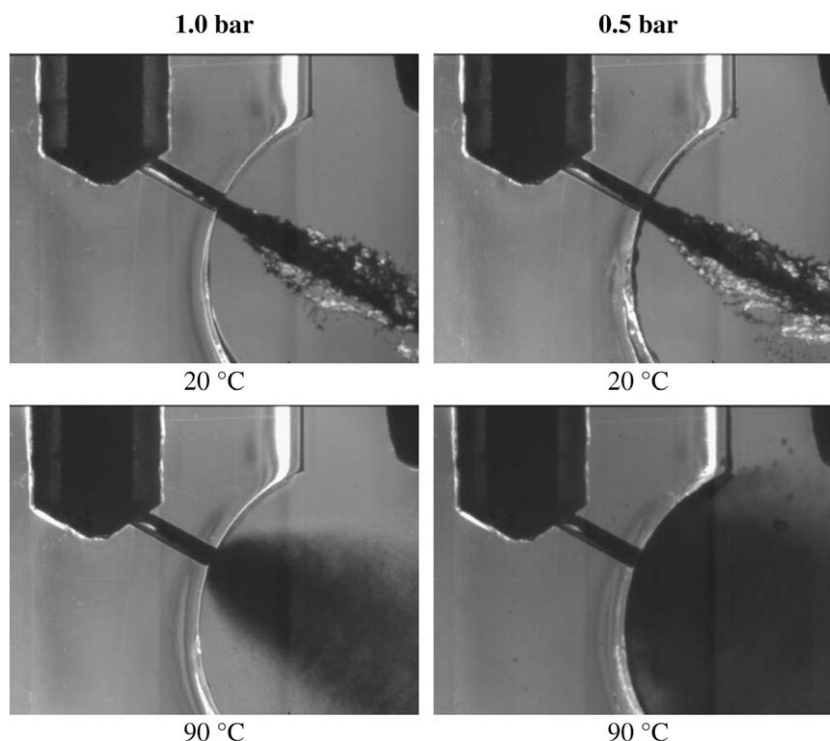


Fig. 15. *n*-Pentane at different pressure and temperature conditions.

boiling remain highly coupled, the process is believed to occur in the following manner: upon release into the low-pressure gaseous atmosphere, micro-bubbles originating from cavitation and, potentially, air entrainment inside the nozzle are thought to act as nucleation sites for the rest of the superheated components which increase the rate at which these can boil. This cascade process continues to the point where vaporisation can be near instantaneous.

Bubble growth and the energy released from bubble rupture, which is transferred to the surrounding liquid is therefore important in the production of new ligaments. In this respect, the surface tension is a critical parameter as it will define the surface energy necessary for bubbles to grow and break-up the spray into smaller ligaments and droplets. Macroscopic images of the spray show the effects of these phenomena on the global spray formation; the spray collapses as a result of the movement of the vaporised fuel towards low-pressure regions below the injector tip. The larger the rate of vaporisation, the greater the extent of spray collapse seen on a macroscopic level. A recent study by Moon et al. [16] also investigated temperature effects on in-nozzle flow and spray formation but used a pressure-swirl atomiser. They too found that although the spray angle was higher near the nozzle exit, the spray collapsed more rapidly when the fuel temperature increased. This was also attributed to smaller droplets due to flash boiling and the movement of these into low-pressure regions below the injector tip.

Having analysed the effects of liquid temperature and gas pressure on cavitation and spray break-up, some interpretation of the different fuel properties is necessary to understand which ones can provide the critical link to atomization efficiency improvements. Clearly there are differences in the vapour pressures (Fig. 2) and in the viscosities, illustrated via the liquid Reynolds number (Fig. 8). The surface tension is not shown here but it is our intention to also consider the Weber number in our study, particularly with respect to ‘matching’ issues between the different fuels. The main differences arise from the vapour pressure and boiling points (Figs. 1 and 2). The viscosities do have a significant effect on the Reynolds number, which is nearly double for *n*-pentane compared to that of *iso*-octane along the plotted temperature range

but although this will affect the levels of cavitation present, the vapour pressures will dictate the behaviour of the fuel as it exits from the nozzle. For example, an increase in fuel temperature increases the vapour pressure, requiring a smaller decrease in static pressure inside the nozzle before the onset of cavitation, *i.e.* increasing the degree of cavitation for a given fuel/gas pressure difference. It follows that the larger degree of superheat by a fuel’s chemical components, the greater the cavitation. Whether there is a particular ‘optimum’ level of cavitation which is sufficient to trigger the rapid disintegration of the spray at low and high temperatures is something that needs further investigation since the application of these injection systems to future engines means that excessive cavitation is not necessarily a good thing all the time; cavitation can limit the flow rate, which is a setback if considering other types of fuels, *e.g.* alcohols that already require longer injection pulse widths at stoichiometry and/or due to their lower energy contents.

4. Summary and conclusions

This work has investigated the main factors affecting spray formation from a multi-hole injector for DISI engine applications. The experiments were carried out in a quiescent pressure chamber. Four types of fuels with different grades of volatility were studied for a range of injector-body temperatures (20–120 °C) and chamber pressures (0.5 and 1.0 bar), *i.e.* for conditions representative of in-cylinder phenomena for injection strategies during the intake stroke of an engine and for injector temperatures representative of typical engine-head temperatures. The tested fuels included a multi-component gasoline and the single components *iso*-octane and *n*-pentane. High magnification imaging of the near-nozzle region was performed using the real injector and a new optical nozzle was designed to investigate the flow phenomena inside the injector.

The in-nozzle flow regime was highly sensitive to the fuel temperature as a result of the vapour pressure and temperature relationships. Outside the nozzle the degree of superheating experienced by the fuels dramatically improves primary break-up and atomization. This is believed to be caused by the presence of va-

pour bubbles which act as nucleation sites for the flashing of low boiling point components and the rapid growth and rupture of such bubbles, which also contribute to the disintegration process of the spray. Other fluid properties such as viscosity and surface tension enhance the effect these processes have on the overall spray formation and break-up. Higher gas pressures act as a damping factor mainly through the effects on vapour pressure or boiling points. The effects are also reflected in the cavitation numbers which predicted operation in the cavitating regime for all the present experimental conditions in the real injector and proven by the optical nozzle work. The main conclusions can be summarised as follows:

- Similar spray formations at near-nozzle locations were seen compared to macroscopic characteristics observed with the real injector at similar test conditions. This indicated that in-nozzle phenomena may have a very significant influence on macroscopic spray development.
- Although higher levels of in-nozzle cavitation are predicted by the calculated vapour pressures, Reynolds and cavitation numbers for gasoline and *n*-pentane relative to *iso*-octane, both the levels of cavitation and the characteristics of spray break-up were observed to be quite similar for all fuels at cold (20 °C) fuel temperature conditions. At hot fuel conditions however, levels of cavitation were higher in general but did not always result in a geometric change in spray formation or faster spray break-up compared with the cold condition.
- For *iso*-octane an increase in fuel temperature to 90 °C increased the levels of in-nozzle cavitation but did not significantly change the primary spray break-up.
- For gasoline an increase in liquid temperature to 90 °C increased the levels of in-nozzle cavitation and resulted in an asymmetric spray at both 0.5 and 1.0 bar gas pressures with the higher spray angle on the same side as cavitation in the nozzle. Spray break-up and atomization efficiency were clearly improved.

- For *n*-pentane the nozzle was nearly completely filled with cavitation at 90 °C and almost instantaneous vaporisation occurred outside the nozzle. Spray break-up was significantly improved and there was a total absence of a liquid core with the spray being clearly two-phase on exit from the nozzle, particularly at 0.5 bar gas pressure.
- At high fuel temperatures, although the higher vapour pressures resulted in more cavitation inside the nozzle hole, it is the level of superheat, *i.e.* the extent to which the liquid temperature is above its boiling point at that gas pressure, that determines the efficiency of atomisation. Cavitation is useful however because it supplies a plentiful source of vapour bubbles which act as nucleation sites to increase the rate at which superheated components in the spray can boil off.
- The biggest effect of gas pressure was in increasing/reducing the effective level of superheating experienced by the fuels through its effect on the boiling point.

The work is currently being extended to include further studies of the effect of fuel properties, mainly viscosity and surface tension, in light of continuing worldwide trends to adopt higher percentage of alcohol fuels. For example ethanol has almost twice the viscosity of gasoline's main constituents at cold conditions and butanol has almost three times the viscosity of ethanol and larger surface tension as well. Additionally, future work will focus on nozzles with 0.2 mm diameter for direct comparison with the results of the present study. Finally, through higher magnification imaging, the transient nature of cavitation will also be investigated in greater detail.

Appendix A

See Figs. A1, A2 and A3.

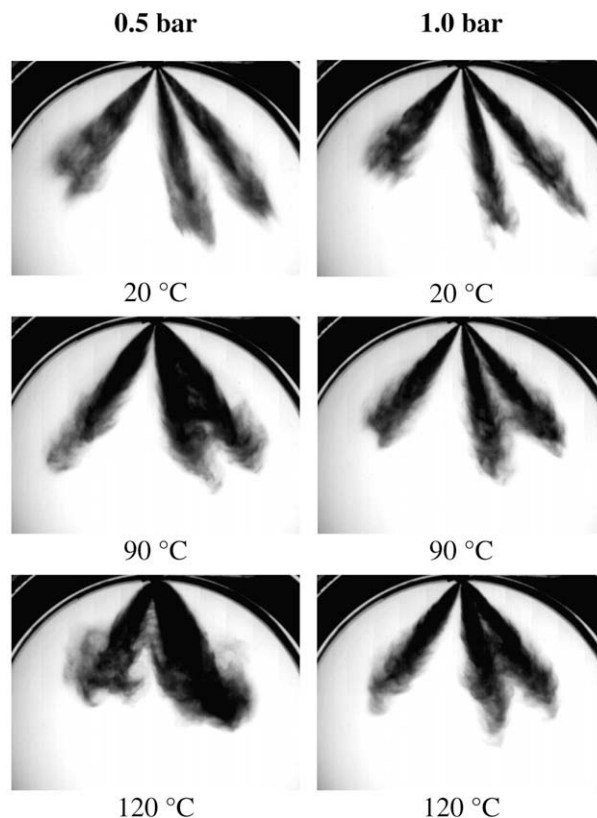


Fig. A1.1. Gasoline spray at 777 μs ASOI.

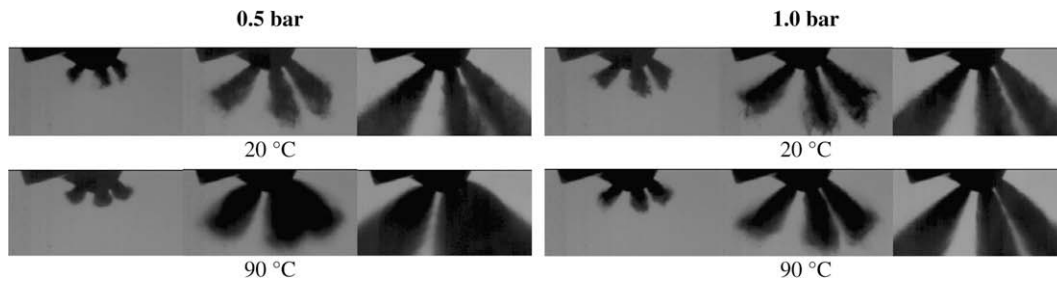


Fig. A1.2. Gasoline near-nozzle imaging at first fuel ' t ', ' $t + 20 \mu s$ ' and steady-state condition.

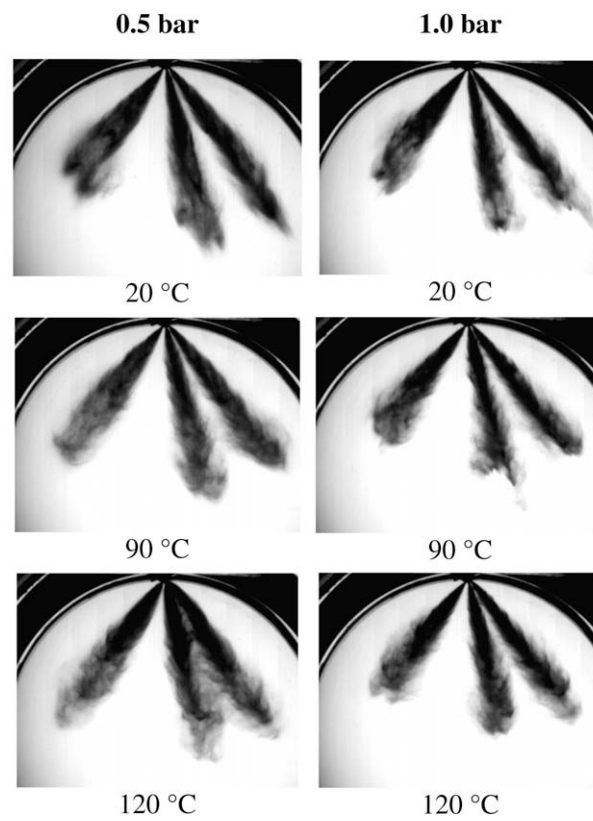


Fig. A2.1. Iso-octane spray at 777 μs ASOI.

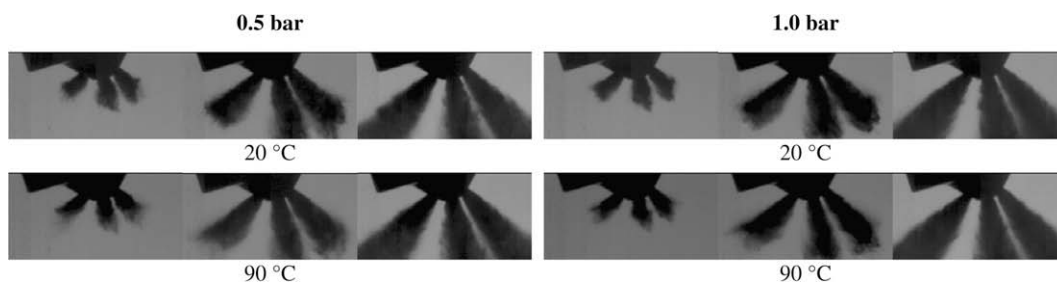


Fig. A2.2. Iso-octane near-nozzle imaging at first fuel ' t ', ' $t + 20 \mu s$ ' and steady-state condition.

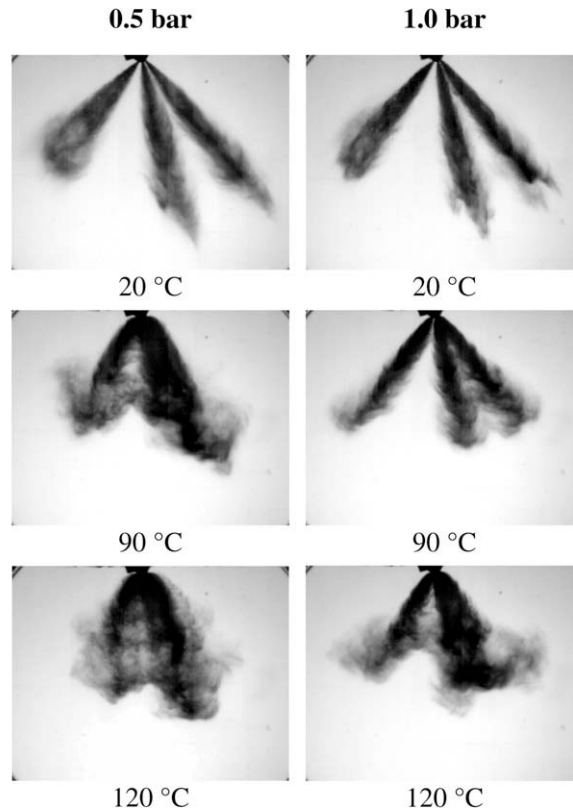


Fig. A3.1. *n*-Pentane spray at 777 μ s ASOI.

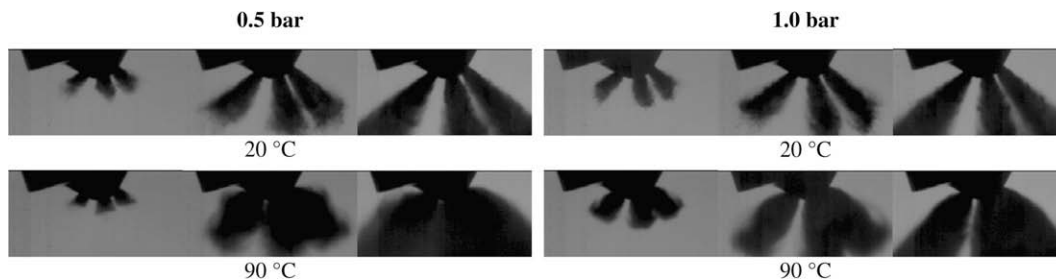


Fig. A3.2. *n*-Pentane near-nozzle imaging at first fuel '*t*', '*t* + 20 μ s' and steady-state condition.

References

- [1] Brennen CE. Cavitation and bubble dynamics. New York: Oxford University Press; 1995.
- [2] Bergwerk W. Flow pattern in diesel nozzle spray holes. Proceedings of IMechE 1959;173(25):655–60.
- [3] Schmidt DP, Corradini ML. The internal flow of diesel fuel injector nozzles: a review. Int J Engine Res 2001;2:1–22.
- [4] Aleiferis PG, Hardalupas Y, Kolokotronis D, Taylor AMKP, Arioka A, Saito M. Experimental investigation of the internal flow field of a gasoline model injector using micro-PIV. SAE Trans J Fuels Lubricant 2006;15(4):597–606 [Paper 2006-01-3374].
- [5] Aleiferis PG, Hardalupas Y, Kolokotronis D, Taylor AMKP, Kimura T. Investigation of the internal flow field of a diesel model injector using PIV and CFD. SAE Paper 2007-01-1897; 2007.
- [6] Chaves H, Knapp M, Kubitzek A, Obermeier F, Schneider T. Experimental study of cavitation in the nozzle hole of diesel injectors using transparent nozzles. SAE Paper 950290; 1995.
- [7] Miranda R, Chaves H, Martin U, Obermeier F. Cavitation in a transparent real size VCO injection nozzle. In: Proceedings of ICLASS, Sorrento Italy; 2003.
- [8] Chaves H, Schuhbauer I. Cavitation in an asymmetric transparent real-size VCO nozzle. Spray'06, Workshop über Sprays, Erfassung von Sprühvorgängen und Techniken der Fluidzerstäubung; 2006.
- [9] Badock C, Wirth R, Fath A, Leipertz A. Investigation of cavitation in real size diesel injection nozzles. Int J Heat Fluid Flow 1999;20:538–44.
- [10] Suh HK, Lee CS. Effect of cavitation in nozzle orifice on the diesel fuel atomization characteristics. Int J Heat Fluid Flow 2008;29:1001–9.
- [11] Walther J, Schaller JK, Wirth R, Tropea C. Characterization of cavitating flow fields in transparent diesel injection nozzles using fluorescent particle image velocimetry (FPIV). In: Proceedings of ILASS-Europe, Darmstadt, Germany; 2000.
- [12] Walther J, Schaller JK, Wirth R, Tropea C. Investigation of internal flow in transparent diesel injection nozzles using fluorescent particle image velocimetry (FPIV). In: Proceedings of ICLASS, Pasadena, USA; 2000.
- [13] Allen J, Hargrave G. Fundamental study of in-nozzle fluid flow and its effect on liquid jet break-up in gasoline direct injectors. In: Proceedings of ILASS-Europe, Darmstadt, Germany; 2000.
- [14] Allen J, Hargrave GK, Khoo YC. In-nozzle and spray diagnostic techniques for real sized pressure swirl and plain orifice gasoline direct injectors. SAE Paper 2003-01-3151; 2003.
- [15] Khoo YC, Hargrave GK. Real-sized pressure swirl GDI injector investigation with HSFV and FPIV. J Phys: Conf Ser 2006;45:77–84 [2nd ICOLAD].
- [16] Moon S, Bae C, Abo-Serie E, Choi J. Internal and near-nozzle flow a pressure-swirl atomizer under varied fuel temperature. Atomiz Spray 2007;17: 1–11.
- [17] Gilles-Birth I, Bernhardt S, Spicher U, Rechs M. A study of the in-nozzle flow characteristics of valve-covered orifice nozzles for gasoline direct injection. SAE Paper 2005-01-3684; 2005.
- [18] Gilles-Birth I, Rechs M, Spicher U, Bernhardt S. Experimental investigation of the in-nozzle flow of valve covered orifice nozzles for gasoline direct injection.

- In: Proceedings of the seventh international symposium on internal combustion diagnostics, Baden-Baden, Germany; 2006. p. 59–78.
- [19] Arcoumanis C, Flora H, Gavaises M, Badami M, Cavitation in real-size multi-hole diesel injector nozzles. SAE Paper 2000-01-1249; 2000.
 - [20] Baz, Champoussin J-C, Lance M, Marie J-L, Investigation of the cavitation in high pressure diesel injection nozzles. In: Proceedings of ASMEFEDSM'02, Montreal, ASME, New York; 2002. p. 425–9.
 - [21] Soteriou C, Andrews R, Smith M, Further studies of cavitation and atomization in diesel injection. SAE Paper 1999-01-1486; 1999.
 - [22] van Romunde Z, Aleiferis PG, Effect of operating conditions and fuel volatility on development and variability of sprays from gasoline direct-injection multi-hole injectors. Atomiz Spray 2009;19:207–34.
 - [23] van Romunde Z, Aleiferis PG, Cracknell RF, Walmsley HL, Effect of fuel properties on spray development from a multi-hole DISI engine injector. SAE Trans J Engine 2007;116(3):1313–31 [SAE Paper 2007-01-4032].
 - [24] Serras-Pereira J, Aleiferis PG, Richardson D, Wallace S, Mixture formation and combustion variability in a spray-guided DISI engine. SAE Trans J Engine 2007;116(3):1332–56 [SAE Paper 2007-01-4033].
 - [25] Serras-Pereira J, Aleiferis PG, Richardson D, Wallace S, Spray development, flow interactions and wall impingement in a direct-injection spark-ignition engine. SAE Paper 2007-01-2712; 2007.
 - [26] Serras-Pereira J, Aleiferis PG, Richardson D, Wallace S, Characteristics of ethanol, butanol, iso-octane and gasoline sprays and combustion from a multi-hole injector in a DISI engine. SAE Int J Fuels Lubricant 2008;1:893–909 [SAE Paper 2008-01-1591].
 - [27] Aleiferis PG, Serras-Pereira J, van Romunde Z, Richardson D, Wallace S, Cracknell RF, Walmsley HL, Optical studies of spray development in a quiescent chamber and in a direct-injection spark-ignition engine. In: Proceedings of the international conference on internal combustion engines: performance, fuel economy and emissions, London, UK; 2007. p. 3–13 [IMechE].
 - [28] Yaws CL, Yaws' handbook of thermodynamic and physical properties of chemical compounds, Knovel; 2003.
 - [29] Bode J, Zum kavitationseinfluss auf den zerfall von flüssigkeitsfreistrahlen, Max-Planck Institut für Strömungsforschung, Diss., Göttingen; 1991.